A High Resolution, Digital, Aerial Photogrammetric Analysis of Historical Shoreline Change and Net Sediment Transport Along the Kihei Coast of Maui, Hawaii

John J. B. Rooney and Charles H. Fletcher, III

Coastal Geology Group
Department of Geology and Geophysics
School of Ocean and Earth Science and Technology (SOEST)
University of Hawaii at Manoa
1680 East-West Road, Post 721
Honolulu, Hawaii 96822

Reprinted from the Proceedings of the Thirteenth Annual National Conference on Beach Preservation Technology, February 2-4, 2000, Melbourne, Florida

A High Resolution, Digital, Aerial Photogrammetric Analysis of Historical Shoreline Change and Net Sediment Transport Along the Kihei Coast of Maui, Hawaii

John J. B. Rooney, Research Assistant
Charles H. Fletcher, Professor

University of Hawaii at Manoa
School of Ocean and Earth Science and Technology (SOEST)
Department of Geology and Geophysics
Coastal Geology Group
1680 East-West Road, Post 721
Honolulu, Hawaii 96822
jrooney@soest.hawaii.edu, fletcher@soest.hawaii.edu

ABSTRACT

This study examines historical shoreline change in southwestern Maui, Hawaii based on orthophotos for seven years between 1949 and 1997 and NOAA T-sheet shorelines from 1900 and 1912. A reweighted least squares (RLS) regression is applied to the most recent trend in the data to calculate average annual erosion hazard rates and delineate the 30 year erosion hazard area.

Historical movement of the vegetation line and beach step crest is used to estimate net sediment transport. Between 1912 and 1949 the southern coastline of the study site receded rapidly, an average of 1.8 m yr^{-1}. In successively later time intervals the focus of erosion migrated northward. Some of the eroded sediment may have been deposited in the northern part of the site, which accreted three times more sediment than was eroded from the south. Significant net sediment transport to the north had occurred by 1912, prior to extensive known anthropogenic disturbance of the shoreline. Net accretion, and timing of the observed changes, suggest natural forcing is primarily responsible. An overall shift from accretion to erosion starting around 1975, and low rates of net sediment transport since then, are primarily due to sediment impoundment from the proliferation of coastal armoring that began in the early 1970s. Beach erosion is a serious problem in Hawaii, as evidenced by the 44% mean decrease in beach width at this site from 1949 to 1997.

INTRODUCTION

Beaches are a tremendously important cultural, recreational, economic, and ecological resource in the state of Hawaii. They are, for example, a vital cornerstone of the visitor industry, which has supported 31 percent of the state's gross product since 1990 (DBEDT, 1999). Despite their importance, beaches on all the main Hawaiian islands are seriously degraded (Makai Ocean Engineering and Sea Engineering, 1991; Sea Engineering, 1988). On the island of Maui it has been estimated that one third of the original sandy beach has been lost or narrowed over the last half century (Fletcher and Hwang, 1994). As a first step toward better protection of their beach resources, coastal zone managers need to have accurate, detailed information about historic patterns of shoreline change (Fletcher and Lemmo, 1999). The research reported here was designed to provide such information for a study site centered on the southwest coast of Maui. Techniques and methodologies developed at this site are now being applied to study all of the significant sandy shoreline areas on Maui to improve understanding of island-wide coastal sediment dynamics.

Study Area

The study area (Figure 1) located in the town of Kihei, Maui extends along 5 km of coastline fronted by a wide fringing reef and terminated to the north by the rock walls of the ancient Hawaiian Koieie Fishpond. The southern end of the reef-fronted area is marked by a small natural rocky headland. South of that are a number of pocket beaches characterizing the remainder of this coastline. The first of these, Kamaole I Beach Park, is also included within our study area. In 1949 the entire stretch of coastline except for the rocky headlands had a relatively wide sandy beach. Since then, 1800 m of the originally sandy shoreline has been replaced by seawalls and revetments.

The site is in the lee of West Maui and the islands of Molokai, Lanai, and Oahu, relative to the large north pacific swells that impact Hawaii every winter. Likewise it is largely protected from chop and swell generated by the brisk northeasterly tradewinds, which occur about 70 percent of the time, particularly in the summer months of May through September (Haraguchi, 1979). The

Figure 1. Halama Study Site

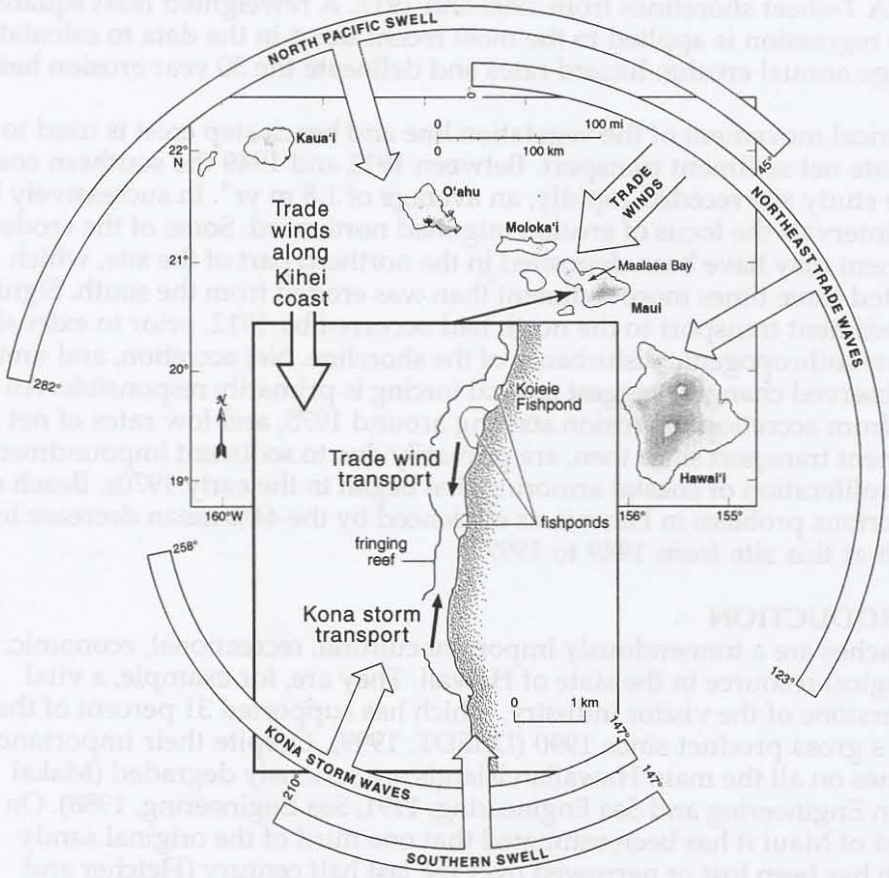

tradewinds on Maui tend to accelerate through the central valley separating the volcanic peaks of West Maui and Haleakala. The winds diverge upon leaving the valley and the air stream that is diverted south along the Kihei coast rises up the sun-heated western slope of Haleakala , forming an ascending spiral of air know as the "Maui vortex" (Schroeder, 1993). Thus the Kihei coastline does experience strong tradewinds, but they are usually from the north (alongshore) rather than from the northeast.

Although somewhat protected by the islands of Lanai and Kahoolawe, the study site is vulnerable to storm and wave events that approach from the south and southwest. South swell, generated by storms in the southern hemisphere, usually impact the Hawaiian Islands in the summer and early autumn. These events typically have wave heights of about 0.3 m to 1.2 m, periods of 14 to 22 seconds (Armstrong, 1983).

Kona winds are stormy, rain-bearing winds that blow from the south or south-southwest. They accompany low pressure systems approaching the islands from the west, and are most common in the late winter and early spring. Kona events can generate wave heights of 3 to 5 m and periods of 8-10 seconds. Although kona winds occur only 10% of the time and are usually light, the occasional strong kona storms have caused extensive damage to south and west facing shorelines, including the Kihei coast (U.S. Army Corps of Engineers, 1967; Makai Ocean Engineering, Inc. and Sea Engineering, Inc., 1991).

METHODS

Historical Shoreline Positions

Historical shoreline positions were acquired from both aerial photographs and NOAA T-sheets. Only 1:12,000 scale or larger, vertical, and survey-quality aerial photographs were used. Photographs meeting these criteria dated from 1949, 1960, 1963, 1975, 1987, 1988, and 1997. Scanned images of the photographs were corrected for distortion errors (Thieler and Danforth, 1994) and mosaicked together following the methodology of Coyne *et al.* (1999). Approximately five ground control points (GCP's) were selected per photograph from the 1997 series. Differential global positioning (DGPS) was used to determine the position of each GCP to within a few millimeters.

Scanned images were imported into commercial rectification software (PCI Geomatics, Inc.). Rectification utilizes the GCP's, the principle point of a photograph, and information about the camera. The process orients an image so that true north is up, assigns it a common map projection (UTM) and datum (WGS84), and rubber sheets it to best fit the GCP's. The middle of a rectified image has better position accuracy than the edges, so only the central third of each image was used when joining rectified images together. A batch of images joined together in this way is then resampled to bring them to a common scale of 0.5 m per pixel. The resulting photomosaic is a georeferenced image of a continuous stretch of coastline.

In rectfying images from years prior to 1997, both GCP's and pass points are used. Pass points are precise features that are visible in both the 1997 photomosaic and the historical image to be rectified. A photomosaic was made for each of the earlier series of photographs. The rectification process is currently the most time consuming part of the entire analysis. We will be investigating an aerotriangluation method and use of rectified satellite images as a means to decrease our production time and improve the accuracy of our photomosaics.

We define the crest of the beach step and the vegetation line as the seaward and landward boundaries of the beach, respectively (Bauer and Allen, 1995), and the horizontal distance between them as the beach width (Figure 3). We track the movement of the beach step crest through time to calculate erosion rates. Coyne *et. al.* (1999) defined the shoreline change reference feature (SCRF) as the beach step crest in their work for the FEMA "Evaluation of Erosion Hazards" study.

Although somewhat protected by the islands of Lanai and Kahoolawe, the study site is vulnerable to storm and wave events that approach from the south and southwest. South swell, generated by storms in the southern hemisphere, usually impact the Hawaiian Islands in the summer and early autumn. These events typically have wave heights of about 0.3 m to 1.2 m, periods of 14 to 22 seconds (Armstrong, 1983).

Kona winds are stormy, rain-bearing winds that blow from the south or south-southwest. They accompany low pressure systems approaching the islands from the west, and are most common in the late winter and early spring. Kona events can generate wave heights of 3 to 5 m and periods of 8-10 seconds. Although kona winds occur only 10% of the time and are usually light, the occasional strong kona storms have caused extensive damage to south and west facing shorelines, including the Kihei coast (U.S. Army Corps of Engineers, 1967; Makai Ocean Engineering, Inc. and Sea Engineering, Inc., 1991).

METHODS

Historical Shoreline Positions

Historical shoreline positions were acquired from both aerial photographs and NOAA T-sheets. Only 1:12,000 scale or larger, vertical, and survey-quality aerial photographs were used. Photographs meeting these criteria dated from 1949, 1960, 1963, 1975, 1987, 1988, and 1997. Scanned images of the photographs were corrected for distortion errors (Thieler and Danforth, 1994) and mosaicked together following the methodology of Coyne *et al.* (1999). Approximately five ground control points (GCP's) were selected per photograph from the 1997 series. Differential global positioning (DGPS) was used to determine the position of each GCP to within a few millimeters.

Scanned images were imported into commercial rectification software (PCI Geomatics, Inc.). Rectification utilizes the GCP's, the principle point of a photograph, and information about the camera. The process orients an image so that true north is up, assigns it a common map projection (UTM) and datum (WGS84), and rubber sheets it to best fit the GCP's. The middle of a rectified image has better position accuracy than the edges, so only the central third of each image was used when joining rectified images together. A batch of images joined together in this way is then resampled to bring them to a common scale of 0.5 m per pixel. The resulting photomosaic is a georeferenced image of a continuous stretch of coastline.

In rectfying images from years prior to 1997, both GCP's and pass points are used. Pass points are precise features that are visible in both the 1997 photomosaic and the historical image to be rectified. A photomosaic was made for each of the earlier series of photographs. The rectification process is currently the most time consuming part of the entire analysis. We will be investigating an aerotriangluation method and use of rectified satellite images as a means to decrease our production time and improve the accuracy of our photomosaics.

We define the crest of the beach step and the vegetation line as the seaward and landward boundaries of the beach, respectively (Bauer and Allen, 1995), and the horizontal distance between them as the beach width (Figure 3). We track the movement of the beach step crest through time to calculate erosion rates. Coyne *et. al.* (1999) defined the shoreline change reference feature (SCRF) as the beach step crest in their work for the FEMA "Evaluation of Erosion Hazards" study.

Where the seaward extent of vegetation is limited by seawalls or revetments, the vegetation line is vectored along the seaward side of the structure. The crest of the beach step is also delineated along the base of coastal armoring where there is no subaerially exposed beach during high tide. On armored shorelines, these features follow the estimated position of the mean high water line (MHWL). Following these definitions, the beach width for armored coastlines that are no longer fronted by sandy beach is zero.

Shoreline position error is calculated as the square root of the sum of the squares of total measurement error, tidal, and seasonal fluctuation of the SCRF. Total measurement error is the square root of the sum of the squares of rectification error, digitizing error, and pixel accuracy (0.5 m). Tidal fluctuation is the maximum horizontal movement of the beach step crest measured between the lowest and highest tides during a spring tide, at several locations. Seasonal fluctuation is calculated from the mean movement of the SCRF at the 95% confidence level between the 1987 (summer) and 1988 (winter) photomosaics.

Topographic Survey Charts

Historical shoreline positions are also acquired from topographic survey charts, or T-sheets. A T-sheet for the northern half of our study site is available from 1900, and one for the southern half, with about 130 m of overlap from 1912. Copies were obtained from a private vendor working with the National Archives, and from the National Ocean Service respectively. The mean high water line (MHWL) from both surveys was digitized on a Summagraphics Microgrid III digitizing pad set at 0.127 mm (0.005 in) resolution, with the operator wearing 2.75 power binocular magnifiers. Triple replicates of each shoreline are made, and the median shoreline position used for analysis.

T-sheets were originally produced in the Old Hawaiian Datum. Digitized T-sheet MHWLs are converted to WGS84 by overlaying with the 1997 photomosaic. MHWLs are shifted seaward a distance equal to the median distance between the median MHWL and the crest of the beach step, as measured from five years of seasonal beach profiles taken within the study site.

As with the photomosaic shorelines, T-sheet shoreline uncertainty is calculated as the square root of the sum of the squares of several terms, including digitizing error and seasonal fluctuations. The tidal fluctuation term is replaced with uncertainty associated with conversion of the MHWL to the beach step crest, and is set at 7 m based on profile data. A term is added also, to account for uncertainty associated with the plotted position of the shoreline on the T-sheet. Its value is set at 5 m from Shalowitz (1964), and confirmed by measurement of offset between prominent rock outcrops and other features common to the T-sheets and 1997 photomosaic.

Erosion Rates

To calculate erosion rates, all historical shorelines are overlain on the 1997 photomosaic and a time series of movement histories calculated every 20 m in the alongshore direction. We determine an end-point rate (EPR) using the earliest and latest shoreline positions (*e.g.*, Foster and Savage, 1989; Dolan *et al.*, 1991). Inspection suggests that the entire study site can be described using 13 sub-cells (Figure 2). The pattern of shoreline change is consistent within a sub-cell, and the pattern is different or distinct from those of neighboring sub-cells. Further inspection of shoreline history reveals that several subcells

display a significant change in shoreline behavior through time. Because they are not well characterized by any single erosion rate we calculate a rate based on the most recent trend in the shoreline, the projected annual erosion hazard rate (AEHR). This is calculated by taking the slope of the reweighted least squares (RLS) regression line fit to the data points included with the most recent trend. Details of the RLS regression are discussed later. For transects experiencing erosion, the AEHR is used to define the 30 year erosion hazard projected from the 1997 vegetation line.

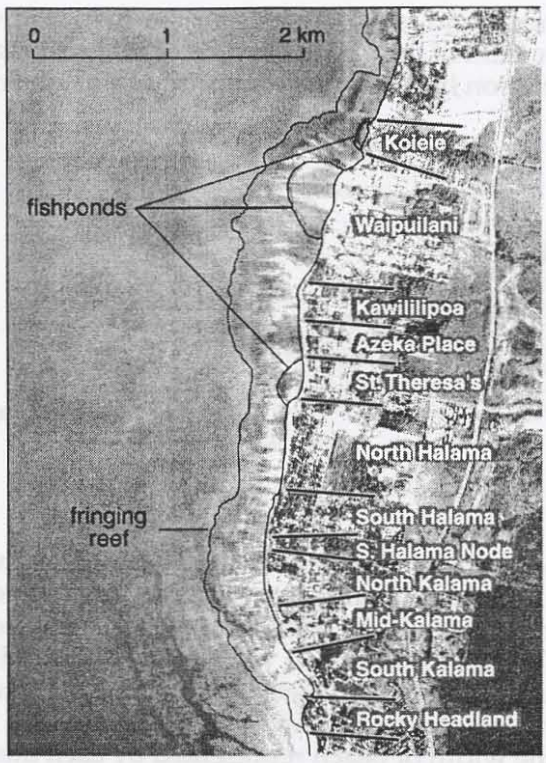

Figure 2. Sub-cells

Volumetric Shoreline Change

As mentioned above, a profile line (one of approximately 90 statewide) established within our study site was surveyed each summer and winter for five years. The profile data are used to develop a model estimating volumetric changes along the coast from historical shoreline movement information (Figure 3). The model, modified from Bodge (1998), uses the change in beach width (ΔX) as a proxy for change in volume under the profile (ΔV) based on the $\Delta V/\Delta X$ relationship determined from our survey data. The slope of a regression line running through the origin and fit to the data yields what Bodge (1998) refers to as the "G_p" value, expressed here as:

$$G_p = \frac{\Delta V}{\Delta X} = \frac{volume\ \ change\ \ per\ \ unit\ \ shorelength}{change\ \ in\ \ beachwidth}$$

The G_p term has units in this case of m^3 per meter of beach width change per meter along the shoreline, or $m^3\ m^{-1}\ m^{-1}$. Given that the profile data was collected each summer and winter over a relatively short (five year) timespan, our G_p value better reflects seasonal variation than it does a long-term trend. The G_p value is multiplied by the change in beach width (ΔX) determined from aerial photo history, to yield a volume change for a 1 m wide strip of the active, sandy beach. This comprises the first term in our volumetric change model.

The second term accounts for the change in volume associated with movement of the vegetation line. It reflects long-term variation in which the vegetation line moves significantly (Morton and Speed, 1998), and is calculated from two measurements. The first, ΔZ, is the elevation difference between the base of the actively changing profile (depth of closure) and the average elevation of the vegetated coastal plain, as seen in the profiles. The second measurement, ΔVeg, is the horizontal distance the vegetation line moves over a given time interval. The ΔZ and ΔVeg measurements are multiplied and define the volumetric change under a 1 m wide strip of the vegetated profile.

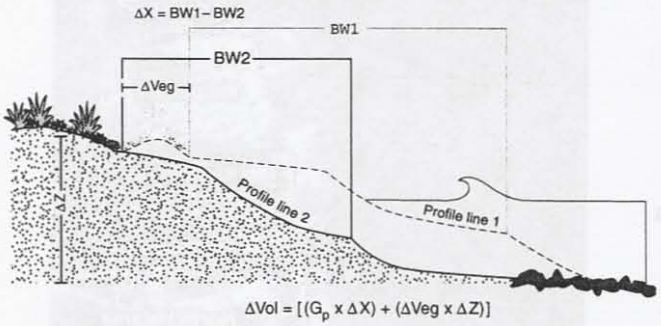

Figure 3. Volumetric Change Model

The change in profile volume ($G_p * \Delta X$) and the change in coastal plain volume ($\Delta Veg * \Delta Z$) together give the total change in volume, ΔVol, under the entire length of a 1 m wide shore-normal line. That result is multiplied by 20 m, the width of beach represented by each measurement of historical shoreline movement. This procedure can be written as:

$$\Delta Vol = [(G_p * \Delta X) + (\Delta Veg * \Delta Z)] * 20 \text{ , in which:}$$

ΔVol = total change in volume for a 20 m wide shore-normal strip
G_p = slope of the best fit line from a plot of $\Delta V/\Delta X$
ΔX = horizontal change in beach width
ΔVeg = horizontal movement of the vegetation line
ΔZ = elevation difference between the coastal plain and the depth of closure, as seen in profile data

Results from the model for the North Halama sub-cell compared well with measurements of volume change in the area. Using the above equation, volumetric changes were calculated for each time increment of our shoreline history at 20 m alongshore spacing, and for each sub-cell.

Sediment Production

The primary components of the beach and nearshore sediment within the study site are calcareous, produced by foraminifera, red algae, mollusks, coral, and echinoids. (Moberly, *et. al.*, 1963). Since all of these organisms can be seen living in the area today, we estimated current rates of *in situ* sediment production. Two different types of reef environment are found at the Halama study site. There is a large reef flat area with low percentages of live coral cover, and a smaller reef slope area with high percentages of live coral cover. The surface area of each is measured from the 1997 photomosaics. Gross calcium carbonate production rates of 1.4 and 7.0 kg m^{-2} yr^{-1} respectively are assigned to the reef flat and slope environments (Harney and Fletcher, 1999). They further estimate that 50% of the gross $CaCO_3$ production is reduced to sediment, and that 50% of that sediment is trapped within the reef

framework. That leaves the remaining 50% potentially available to add to the beach sediment reservoir. The highest production rates are found on the reef slope, which is on the outer edge of the reef platform. Once a sand grain falls over the outer edge of the reef platform it will be quite difficult for it to be redeposited on the reef platform. We estimate therefore that 50% of the sediment produced and not trapped within the reef framework is removed from the reef system by transport off the edge of the reef platform. The remaining 50%, or 12.5% of the gross $CaCO_3$ production, is estimated to be added to the beach system. Total sediment production for the entire reef area fronting the study site was estimated for the time period between 1900 and 1997 and compared to the volumetric shoreline changes estimated above.

RESULTS

Although linear rates of shore and vegetation line movement and their associated volumetric changes are calculated at a 20 m spacing, for ease of interpretation, results tabulated below are for the 13 study site sub-cells.

Table 1. Net, mean shoreline movement for each sub-cell and interval of time, in meters. Missing numbers indicate lack of T-sheet coverage for that sub-cell and time interval. Negative numbers indicate erosion.

Interval /Sub-cell	1900 -1912	1912 -1949	1900 -1949	1949 -1960	1960 -1963	1963 -1975	1975 -1988	1988 -1997	Mean
Koieie	-	-	17.9	-30.2	-11.2	6.3	-13.3	3.5	-4.5
Waipuilani	-	-	45	3.9	-1.0	5.3	-11.0	-0.3	7.0
Kawililipoa	23.2	20.7	29.8	11.3	-0.9	11.6	5.4	-0.1	7.4
Azeka Pl.	-	16	-	14.8	-1.5	5.6	1.8	-0.7	6.0
St. Theresa	-	14.2	-	8.8	2.9	-9.4	-0.3	4.7	3.5
N. Halama	-	15.6	-	8.5	4.1	7.0	-9.2	-5.9	3.4
S. Halama	-	-2.4	-	-6.5	1.7	-4.8	-9.3	-1.2	-3.8
S Hal Node	-	-15.6	-	-3.0	-0.6	-1.5	-6.4	-2.8	-5.0
N Kalama	-	-12.1	-	-5.0	-11.5	-0.8	-5.9	-3.6	-6.5
M Kalama	-	-39.0	-	12.4	-3.1	9.9	-8.8	-4.2	-9.6
S. Kalama	-	-66.0	-	-5.5	6.7	6.9	-8.9	-1.6	-11.4
Rocky Area	-	-16.6	-	-5.3	-3.7	5.5	-5.5	-0.7	-4.4
Kamaole I	-	-1.9	-	-9.1	-24.1	38.6	-10.0	-3.5	-1.7
Totals	23.2	-5.7	30.9	-2.3	-3.3	6.2	-6.3	-1.3	-1.2

Table 2. Mean long-term (End Point Rate) and annual erosion hazard rates (AEHRs) for each sub-cell, in m yr^{-1}. Negative numbers indicate erosion.

Interval /Sub-Cell	End Point Rates	AHERs
Koieie	-0.619	-0.792
Waipuilani	0.567	-0.418
Kawililipoa	0.763	0.346
Azeka Pl.	0.252	0.232
St. Theresa's	0.230	0.038
N. Halama	0.231	-0.746
S. Halama	-0.276	-0.511
S. Hal. Node	-0.350	-0.336
N. Kalama	-0.482	-0.725
Mid Kalama	-0.741	-0.865
S. Kalama	-0.895	-0.188
Rocky Area	-0.311	-0.163
Kamaole I	-0.119	-0.617
Overall Means	-0.135	-0.365

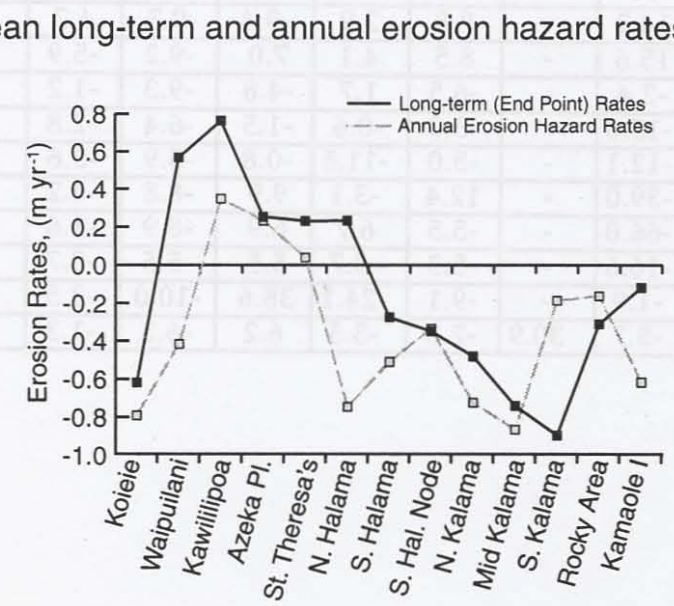

Figure 4. Mean long-term and annual erosion hazard rates (AEHRs) for each sub-cell, in m yr^{-1}. Negative numbers indicate erosion.

Table 3. Mean beach width for each sub-cell and year of photographic coverage, in m. The last column shows the overall change in beach width between 1949 and 1997. Negative values indicate erosion.

Year / Sub-Cell	1949	1960	1963	1975	1988	1997	Change 1997-1949
Koieie	26.7	54.2	21.1	21.0	2.1	6.5	-20.2
Waipuilani	20.7	19.9	20.5	19.4	14.6	15.0	-5.6
Kawililipoa	15.0	15.8	13.0	15.9	13.1	10.2	-4.8
Azeka Pl.	17.8	12.3	17.0	14.3	14.8	14.5	-3.3
St. Theresa	24.4	14.1	22.1	18.9	15.6	14.7	-9.7
N. Halama	17.4	16.9	16.6	16.6	11.6	7.0	-10.4
S. Halama	16.4	12.6	18.0	10.8	0.0	0.0	-16.3
S Hal Node	15.6	13.0	14.3	11.0	5.5	5.8	-9.8
N. Kalama	19.0	16.7	12.9	6.8	1.9	0.0	-18.9
Mid Kalama	18.4	15.6	19.3	9.2	1.0	0.0	-18.3
S. Kalama	14.9	10.8	18.6	9.9	1.4	1.7	-13.3
Rocky Area	18.6	10.9	9.8	15.7	3.4	3.5	-15.1
Kamaole I	31.3	38.5	14.1	43.0	42.9	35.5	4.2
Mean	19.7	19.3	16.7	16.3	9.9	8.8	-10.9

Table 4. Volumetric change, or net sediment transport, for each sub-cell and time interval, in units of 10^3 m^3. Shaded boxes track movement of an erosion "hotspot." Boxes with bold outlines illustrate impacts of kona storms.

Interval /Sub-cell	1900 -1912	1912 -1949	1900 -1949	1949 -1960	1960 -1963	1963 -1975	1975 -1988	1988 -1997	Total
Koieie	-	-	-12.1	-14.0	2.4	4.6	-1.5	-4.4	-25.1
Waipuilani	-	-	17.7	12.8	6.5	16.1	-19.3	-2.4	185.3
Kawililipoa	11.0	13.6	20.2	33.0	4.6	27.1	17.6	5.0	132.1
Azeka Pl.	-	6.9	-	17.9	-2.0	-5.5	2.7	2.3	22.3
St. Theresa	-	28.5	-	1.7	-10.4	1.4	-1.9	6.9	26.1
N. Halama	-	35.1	-	24.6	12.2	19.6	-14.2	-6.2	71.0
S. Halama	-	-2.5	-	-4.4	-3.3	1.3	-0.8	-1.5	-11.2
S Hal Node	-	-6.4	-	-0.5	-0.8	0.6	-1.0	-1.5	-9.6
N Kalama	-	-16.4	-	-5.3	-14.2	7.0	-3.5	-3.6	-35.9
M Kalama	-	-43.8	-	-13.7	-7.7	24.8	-2.9	-4.5	-47.8
S. Kalama	-	-49.9	-	-1.2	0.3	12.3	-2.1	-1.6	-42.1
Rocky Area	-	-14.6	-	0.9	-3.1	0.7	4.9	-0.8	-11.9
Kamaole I	-	-3.1	-	-30.2	-8.9	30.9	-20.1	5.0	-26.6
Totals	2.2	-52.6	179.8	21.7	-24.4	140.9	-42.2	-7.4	226.7

In estimating sediment production on the surface of the reef, the area of the reef characterized as "reef slope" covers 0.459 km^2 and is assigned a gross $CaCO_3$ production rate of 7.0 kg m^{-2} yr^{-1}. The area characterized as "reef flat" encompasses 1.279 km^2 and is assigned a production rate of 1.4 kg m^{-2} yr^{-1}. Annually the entire reef is estimated to produce 0.36 kg m^{-2}, 2.5 x 10^6 kg, or approximately 530 m^3 of sediment that is potentially available to the beach

system. That yields a total production of approximately 50,000 m^3 over the 97 year period covered by this study.

DISCUSSION

SCRF

We use the crest of the beach toe as our SCRF for several reasons. It is almost always present in Hawaiian beach systems and is often the only feature other than the vegetation line that is visible in the aerial photographs. Tracking movement of the vegetation line along developed shorelines in Hawaii can be problematic. For example, at many locations within this study site the vegetation line has been artificially stabilized behind coastal armoring while the beach in front has gradually disappeared. Analysis of movement of the vegetation line in these areas would erroneously suggest that the coastline is stable. It has been recommended (Morton and Speed, 1998) that shoreline features sensitive to shore-term fluctuations in sea-level, including the high water line (HWL), not be used to monitor shoreline position. They suggest the use of features which more closely follow the long-term movement of the shoreline. For these reasons listed above, and because this particular project is geared towards monitoring of the condition of the beach as well as overall shoreline movement, we have chosen to use the beach step crest as our SCRF. See Coyne *et al.* (1999) for a further discussion of this topic.

T-sheets

There has been discussion in the literature over the advantages and disadvantages of including data from T-sheets in studies of shoreline change. The primary argument against their use has been that their accuracy is questionable (Smith and Zarillo, 1990; Dolan, *et. al.*, 1980). It has been pointed out by others that the modest increase in position uncertainty that is incurred by using T-sheets is more than offset by the benefits realized from the greater temporal coverage they provide (Crowell *et. al*, 1993; National Research Council, 1990). Particularly large position uncertainty, 14.3 m for most of the study site, results from digitizing at the 1:20,000 scale of the 1912 T-sheet. Position uncertainty from the 1900 T-sheet, at a scale of 1:10,000, is 11.9 m for most of the study site, compared to 8.1 m for shoreline positions derived from photographs. However, including T-sheets at this site is quite useful as they double the time period covered and reveal significant shoreline changes that preceded aerial photographic coverage.

Erosion Rates

A number of methods have been used to calculate erosion rates from historical shoreline position data. Some of the more complex methods such as the Minimum Descriptor length (MDL) criterion (Fenster *et. al.*, 1993) and the Average of Rates (AOR) technique (Foster and Savage, 1989) show promise. However, linear regression has been found to be the best overall method by several researchers (Crowell, *et. al.*, 1999; Crowell, *et. al.*, 1997) and suggested to be the method of choice in some situations by others (Dean and Malakar, 1999; Dolan, *et. al.*, 1991). Agreeing with their assessments, we elected to use linear regression for calculating projected future erosion hazard rates.

The least-squares (LS) method is by far the most common method of linear regression and is the specific technique discussed in the literature referenced above. It works quite well for normally distributed data and has a number of statistical tests associated with it. However, the susceptibility of the LS method to outliers and point clustering or uneven point distribution is well documented with respect to shoreline change analysis (Fenster *et. al.*, 1993;

Dolan, *et. al.*, 1991; Foster and Savage, 1989). To help alleviate this problem we used the reweighted least squares (RLS) regression method, described by Rousseeuw (1990) and outlined below. The first step involves identifying outliers using a least median of squares (LMS) regression. Unlike the trend from LS regressions, which can be thrown off by a single bad data point, an LMS regression is very resistant to outliers, with a breakdown point of 50%. In other words, half of the data used in an LMS regression has to be contaminated before the trend is affected.

Because the LMS method does not explicitly deal with each data point, it is not considered to be analytical and does not include a means to calculate statistics such as confidence limits. The RLS technique takes advantage of the robustness of LMS regression and the standardized statistical tests available for LS regression. It normalizes the LMS residuals by the estimated standard deviation. These standardized residuals, if larger than 2.5, are considered to be outliers. Outliers are assigned a weight of zero, and the remaining "good" data a weight of one. An LS regression is then fit that minimizes the weighted residuals in a least squares sense. It is essentially an LS regression on the "good" data only. We calculate uncertainties for RLS-derived erosion rates using the 80% confidence intervals for the slope, as suggested by Douglass *et. al.* (1999).

As mentioned above, there is a significant change in the shoreline trend for many transects. Some, for example, show a moderate trend of accretion followed abruptly by erosion. Many researchers recommend using the longest available record for calculating erosion rates, provided there have not been physical changes in the system, such as construction of coastal armoring or inlets opening or closing (Crowell, *et. al.*, 1997; Crowell, *et. al.*, 1993; Dolan, *et. al.*, 1991; Leatherman and Crowell, 1997). It has also been pointed out, in particular by Fenster *et. al.* (1993), Morton (1991), and Foster and Savage (1989), that an observed change in trend may in fact reflect a fundamental change in the sediment dynamics of the system rather than a short term fluctuation in the long term trend. This may be the case, whether or not a specific physical change can be cited to explain the change in shoreline trend.

For the study site, a decision was made to use only the most recent trend in the data to calculate projected AEHRs. The island has been experiencing approximately 2.5 mm yr^{-1} of relative sea-level rise (RSLR) for the last several decades. Although local conditions frequently overwhelm the effect of RSLR at decadal timescales, net RSLR should at some point lead to a shift in the equilibrium position of the shoreline. Also, the armoring of an extensive portion of the coastline resulted in artificial impoundment of coastal sand resources. This contributes to sediment deficiencies on the shoreface, loss of the beach in front of these structures where there is net shoreline recession, and a sediment starved system. These physical attributes of the site dictate the need to use only data that reflect the current recessional nature of the shoreline when calculating AEHRs.

Coastal Armoring

A number of measurement points overlay coastal armoring structures during our photo coverage period. We frequently find the dry sandy beach fronting these structures has disappeared and did not reappear in subsequent photographs. Data following the year when the beach first disappeared were discarded from erosion rate calculations. Unless the shoreline trend reverses, the remaining sandy profile will be scoured deeper and the area will develop a sand deficit. A sand renourishment effort would

then require a significant volume of sand to be added to the system before any dry beach at all could reappear.

Beach width

Movements of both the vegetation line and beach step crest are followed to examine changes in beach width. Beach widths, one measure of the well being of a sandy beach, are shown in Table 3 and highlight the severity of the beach loss problem on Maui. Between 1949 and 1997 the mean beach width decreased by 55%, with the largest decrease, 33%, occurring between 1975 and 1988. The widespread construction of coastal armoring in the study site in the early 1970's caused artificial impoundment of sediment landward of the structures and is primarily responsible for the decrease after 1975.

When a sub-cell gains sediment at the shoreface, it's beachwidth increases, as can be seen in many instances in Table 3. If the accreted material remains there for several years it may stabilize the back beach area enough that the vegetation line will be able to move seaward. A similar time lag may occur when a beach is experiencing chronic erosion because the vegetation line will not move landward as rapidly as the beachstep crest (Morton and Speed, 1988). In an undisturbed system the beach will eventually return to its equilibrium width (Coyne *et. al.*, 1996). Natural retreat of the vegetation line is often impeded in Hawaii by landscaping effforts of property owners (Fletcher *et. al.*, 1997) and contributes to long-term beach loss at the site.

Volumes

Table 4 shows patterns of mean volume change, or net sediment transport, by sub-cell and time interval. The northern half of the study site accreted 4.37 x 10^5 m^3 between 1900 and 1997 while the southern half lost 1.85 x 10^5 m^3. Within the reef-fronted portion of the site there was three times more accretion than erosion, despite erosion in the south that was quite severe in some areas. The South Kalama sub-cell lost about 50 x 10^5 m^3 of sediment between 1912 and 1949, or 6.1 m^3 per alongshore meter of shoreline per year (i.e., -6.1 m^3 m^{-1} yr^{-1}). We speculate that some of the sediment eroded from the southern end of the study site was redeposited in the northern part by kona storm processes. Redeposition may have occurred as far south as the North Halama sub-cell, which accreted 1.4 m^3 m^{-1} yr^{-1} between 1912 and 1949. The area of overlap between the 1900 and 1912 T-sheets in the Kawililipoa sub-cell was already experiencing high accretion rates (6.7 m^3 m^{-1} yr^{-1}), suggesting that the area to the south was also experiencing erosion at this time. This is prior to the onset of significant coastal development in the area, or other known anthropogenic factors that might contribute to coastal erosion.

The "hotspot" of erosion at South Kalama gradually moved north, as seen in the shaded boxes in Table 4. As it migrated, areas close to the hotspot changed mode from accreting to eroding. By the late 1960s and especially the early 1970s, as erosion moved north, seawall and revetment construction followed. By artificially impounding coastal plain sediment, these structures cut off this sediment supply to the beach (Fletcher *et. al.*, 1997), resulting in overall erosion and smaller rates of sediment transport throughout the site after 1975. Today the focus of erosion is in the North Halama sub-cell, almost 2 km north of its original location.

A series of major kona storms between 1960 and 1963 caused general erosion during this time, especially on portions of the study site more exposed to southwesterly waves. The kona events also induced significant south-to-north longshore transport, at least 6.6 m^3 m^{-1} yr^{-1}, as evidenced by the impoundment of sediment, on the updrift side of the Halama groin in the

North Halama sub-cell. Concurrent erosion occurred on the downdrift side, in the St. Theresa's sub-cell (see boxes outlined in bold in Table 4).

The walls of Koieie Fishpond show a similar pattern during the 1960-1963 period of high kona storm activity, with the southern side accreting about 15 m while the north side eroded about 12 m. In 1900 however the situation was reversed, with the shoreline north of the fishpond extending about 90 m further seaward than the shoreline to the south. This suggests that the dominant longshore transport that shaped that part of the coast prior to 1900 was southerly. By 1997 the offset had been reduced to less than 15 m, while 200 m south of the fishpond the coastline has prograded 100 m seaward. The bulk of the accretion on the south side of the fishpond occurred between 1900 and 1949.

Southwesterly kona storm waves move significant volumes of sediment northward along the coast, but a similar high volume mechanism is not known to work in the opposite direction. Within Maalaea Bay on the leeward side of the island, the site is not exposed to large waves, except from the south and southwest. The limited fetch in Maalaea Bay north and northwest of the fishpond preclude the generation of large waves in the Bay itself that could move significant volumes of sediment to the south. Tradewind conditions however can and do move smaller volumes of sediment to the south within the site on a day-to-day basis.

We hypothesize that the patterns of shoreline change reflect a dominant direction of longshore transport to the south that persisted for some significant period of time prior to 1900. The direction reversed, at least by 1912 and perhaps as early as shortly before 1900. We further speculate that some climatic shift, that perhaps affected the ratio of tradewind strength and persistence to kona storm activity, may be responsible and may be the simplest explanation that fits these observations. Ongoing research will investigate this hypothesis.

Annual *in situ* sediment production, 530 m^3, is small relative to the volume of sediment transported along the coast. It is only about 3% of the mean volume of sediment transported into or out of an average sub-cell over a single time interval. Over the 97-year period covered by the study, *in situ* production accounts for 18% of the net sediment accumulation. On time scales of years to a century, sediment transport processes are predominate shapers of the coastline. On scales of hundreds to thousands of years however, sediment production is responsible for creating the beach and becomes a very important geologic process.

CONCLUSIONS

Methodological

Taken as a whole, we found the methods presented here to be an effective way to delineate and analyze shoreline changes on scales of years to a century. A faster way to complete photograph rectification would significantly enhance the overall process and is currently being investigated. The use of T-sheets to extend the period covered by the study greatly enhanced our understanding of the coastal processes and history, despite the greater uncertainty associated with the decrease in position control.

No single erosion rate statistic was found to do an adequate job of characterizing past shoreline changes and projecting future erosion hazards in this area. The RLS method of linear regression was found to be more satisfactory than the more common LS regression for determining trends. Although returning very similar results in a majority of cases, the RLS method

was more resistant to outliers while still allowing use of the same statistical tests available for LS regressions.

Tracking of both the beach step crest and vegetation line made it possible to measure changes in beach width and use a two-term model for estimating volumetric change from historical shoreline positions. The model's second term accounts for volume change of the vegetated coastal plain. In conjunction with the first term, which considers volume change of the sandy beach, this model is more accurate than the single-term version and useful for seasonal to century timescales.

Seasonal fluctuation of the shoreline was quantified and found to be the largest consistent source of position uncertainty. Seasonal changes along the shoreline were found to be too random to be easily compensated and must be taken into account when calculating shoreline position error.

We agree with other investigators that, given the dynamic nature of the shoreline and temporal scarcity of shoreline position data, changes must be carefully analyzed. This is true for adequately characterizing past erosion rates, and especially for projecting future erosion hazard areas. Techniques used must be adapted for specific areas and data available.

Area Specific

A major focus of erosion has been migrating northward along the coast, almost 2 km over the past 85 years. Unexpectedly, within the reef-fronted area forming the primary focus of our study, there has been three times more accretion in the northern part than erosion in the south. This behavior started prior to known significant human alteration of the system, and there has been net accretion, suggesting natural rather than anthropogenic forcing is primarily responsible. Climatic changes such as the ratio of tradewind to kona storm activity are hypothesized to be causative factors. Net erosion since 1975, and smaller rates of net sediment transport, are primarily due to anthropogenic impacts. Specifically, sediment impoundment landward of coastal armoring is contributing to a sediment starved system, which has also resulted in a 55% decrease in beach width since 1949.

Future plans include expanding the study to include all the significant sandy shoreline areas on Maui. It is anticipated that comparison of changes between different areas will help to identify the major processes responsible for the dramatic changes that continue to occur along the coast of Maui.

ACKNOWLEDGMENTS

The authors thank Drs. Bruce Richmond, Abby Sallenger, Paul Wessel and Kevin Bodge for their assistance. Additional thanks go to the Coastal Geology Group of the University of Hawaii and geologists from the USGS for their assistance with data collection. This project was funded in part the US Atmospheric Administration Coastal Services Center (NOAA Award No. NA960C0308), the State of Hawaii Department of Land and Natural Resources Main Hawaiian Islands – Marine Resources Initiative (Award No. 432545), and the Hawaii Sea Grant College (Award R/EP 12). SOEST contribution number 4991.

REFERENCES

Armstrong, R.W., 1983. *Atlas of Hawaii*. University of Hawaii Press, Honolulu, 238 p.

Bauer, B.O. and Allen, J.R., 1995. Beach Steps: An Evolutionary Perspective. *Marine Geology*, 123, 143-166.

Bodge, K.R., 1998. Sediment Management at Inlets/Harbors. In: U.S. Army

Corps of Engineers, *Coastal Engineering Manual*, Part V, Ch. 6. Draft, January, 1998.
Coyne, M.A., Fletcher, C.H., and Richmond, B.M., 1999. Mapping Coastal Erosion Hazard Areas in Hawaii: Observations and Errors. *Journal of Coastal Research*, Special Issue No. 28, 171-184.
Coyne, M.A., Mullane, R.A., Fletcher, C.H., and Richmond, B.M., 1996. Losing Oahu: Erosion on the Hawaiian Coast. *Geotimes*, 41(12), 23-26.
Crowell, M., Douglas, B.C., and Leatherman, S.P., 1997. On Forecasting Future U.S. Shoreline Positions: A Test of Algorithms. *Journal of Coastal Research*, 13(4), 1245-1255.
Crowell, M., Honeycutt, M., and Hathewas, D., 1999. Coastal Erosion Hazards Study: Phase One Mapping. *Journal of Coastal Research*, Special Issue No. 28, 10-20.
Crowell, M., Leatherman, S.P., and Buckley, M.K., 1993. Shoreline Change Rate Analysis: Long Term Versus Short Term Data. *Shore and Beach*, 61(2), 13-20.
DBEDT, 1999. *State of Hawaii Data Book: 1999: A Statistical Abstract*. Department of Business, Economic Development and Tourism, Honolulu: 718 p.
Dean, R.G. and Malakar, S.B., 1999. Projected Flood Hazard Zones In Florida. *Journal of Coastal Research*, Special Issue No. 28, 85-94.
Dolan, R., Fenster, M.S., and Holme, S.J, 1991. Temporal Analysis of Shoreline Recession and Accretion. *Journal of Coastal Research*, 7(3), 723-744.
Dolan, R., Hayden, B.P., May, P., and May, S., 1980. The Reliability of Shoreline Change Measurements from Aerial Photographs. *Shore and Beach*, 48, 22-29.
Douglass, S.L., Sanchez, T.A., and Jenkins, S., 1999. Mapping Erosion Hazard Areas in Baldwin County, Alabama and the Use of Confidence Intervals in Shoreline Change Analysis. *Journal of Coastal Research*, Special Issue No. 28, 95-105.
Fenster, M.S., Dolan, R., and Elder, J.F., 1993. A New Method for Predicting Shoreline Positions from Historical Data. *Journal of Coastal Research*, 9(1), 147-171.
Fletcher, C.H. and Hwang, D.J., 1994. *Shoreline Certification Review and Recommendations*:. Office of State Planning, Coastal Zone Management Program, Honolulu: 76 p.
Fletcher, C.H. and Lemmo, S.J., 1999. Hawaii's Emergent Coastal Erosion Management Program. *Shore and Beach*, 67(4), 15-20.
Fletcher, C.H., Mullane, R.A., and Richmond, B.R., 1997. Beach Loss Along Armored Shorelines on Oahu, Hawaiian Islands. *Journal of Coastal Research*, 13(1), 209-215.
Foster, E.R. and Savage, R.J., 1989. Methods of Historical Shoreline Analysis. In Magoon, O.T., Converse, H., Miner, D., Tobin, L.T., and Clark, P. (eds.). *Coastal Zone '89*, American Society of Civil Engineers, 5, 4434-4448.
Haraguchi, P., 1979. *Weather in Hawaiian Waters*. Honolulu: Hawaii Reprographics, 107 p.
Harney, J.N. and Fletcher, C.H., 1999. Carbonate Sediment Budget of a Windward Fringing Reef, Hawaiian Islands. American Geophysical Union Fall Meeting, San Francisco, December, 1999.
Leatherman, S.P. and Crowell, M., 1997. Beach Erosion Trends and Shoreline Forecasting. *Journal of Coastal Research*, 13(4), iii-iv.

Makai Ocean Engineering, Inc., and Sea Engineering, Inc., 1991. *Aerial Photograph Analysis of Coastal Erosion on the Islands of Kauai, Molokai, Lanai, Maui and Hawaii*. Office of State Planning, Coastal Zone Management Program. Honolulu, 200 p.

Moberly, R., Cox, D, Chamberlain, T., McCoy, F.W., and Campbell, J.F., 1963. *Coastal Geology of Hawaii*. Hawaii Institute of Geophysics Report No. 41, Honolulu, 216 p.

Morton, R.A., 1991. Accurate Shoreline Mapping: Past, Present, and Future. In: Kraus, N.C. (ed.), *Coastal Sediments '91*, New York: American Society of Civil Engineers, 997-1010.

Morton, R.A. and Speed, M., 1998. Evaluation of Shorelines and Legal Boundaries Controlled by Water Levels on Sandy Beaches. *Journal of Coastal Research*, 14(4), 1373-1384.

National Research Council, 1990. *Managing Coastal Erosion*. Washington, D.C.: National Academy Press, 182 p.

Rousseeuw, P.J., 1990. Robust Estimation and Identifying Outliers. In: Wadsworth, H.M. (ed.), *Handbook of Statistical Methods For Engineers and Scientists*. McGraw Hill, New York.

Schroeder, T., 1993. Climate Controls. In: Sanderson, M. (ed.), *Prevailing Tradewinds*. University of Hawaii Press, Honolulu, 126 p.

Sea Engineering, Inc., 1988. *Oahu Shoreline Study*. City and County of Honolulu, Department of Land Utilization, Honolulu, 61 p.

Shalowitz, A.L., 1964. *Shore and Sea Boundaries, Volume 2*. U.S. Department of Commerce, Publicatin 10-1, US. Government Printing Office, Washington, D.C., 749 p.

Smith, G.L. and Zarillo, G.A., 1990. Calculating Long-Term Shoreline Recession Rates Using Aerial Photographic and Beach Profiling Techniques. *Journal of Coastal Research*, 6(1), 111-120.

Thieler, R.E., and Danforth, W.W., 1994. Historical Shoreline Mapping (I): Improving Techniques and Reducing Positioning Errors. *Journal of Coastal Research*, 10(3), 549-563.

U.S. Army Corps of Engineers, 1967. *Detailed Project Report, Shore Protection, Kihei Beach, Maui, Hawaii*. Honolulu, 67 p.